Monte Carlo simulations of a single polymer chain under extension above and below the Θ temperature

M. Wittkop, S. Kreitmeier, and D. Göritz
Universität Regensburg, Institut für Experimentelle und Angewandte Physik, D-93040 Regensburg, Germany
(Received 14 August 1995)

The deformation behavior of a single three-dimensional polymer chain above and below the Θ temperature was studied using the bond-fluctuation model. Whereas above the Θ temperature only slight differences to the athermal (infinite temperature) limit occurred, the deformation behavior below the Θ temperature was found to be completely different. The deformation is represented by a coil-strand coexistence and is therefore inhomogeneous. During the coil-strand coexistence the retractive force is independent of the extension. At large strains the coil-strand system becomes unstable; this instability was monitored by the computation of several properties.

PACS number(s): 36.20.−r, 87.15.−v, 83.20.Jp

I. INTRODUCTION

The mechanical properties and deformation behavior of polymers have attracted much attention in polymer physics. It would be desirable to understand the microscopic mechanisms of the deformation process. However, in most cases a complete theoretical description is not possible. Also experiments are limited in exploring microscopic details of deformation processes. In this situation computer simulations are a rather simple and reliable method to get some insight into the deformation behavior. In this paper we will focus on three-dimensional single isolated polymer chains, which can be seen as chains in a very dilute solution.

Most former work concentrated on ideal chains without long-range interactions, i.e., random walks. The force dependence on the end-to-end distance was described by an inverse Langevin function [1–3]. Weiner and Perchak discussed the differences between rigid and flexible chain models [4,5] as well as the influence of quantum calculations [6]. Both theoretically and within computer simulations Weiner and Berman [7,8] studied bond forces in the backbone and fluctuations of axial forces in time. Recently Davis [9] presented a molecular-dynamics simulation of Kuhn and Grün chain segments and discussed anisotropy effects. In recent years extensions and generalizations of the ideal chain were presented by Altenberger, Rosa, and Dahler [10] and by Glatting, Winkler, and Reineker [11–13].

The situation for chains with excluded volume, i.e., self-avoiding walks, is more complicated since this long-range interaction cannot be treated easily. The dependence of the end-to-end distance on the force, projected on the force direction, is quite different from the Langevin function [14,15]. Within a simulation Webman, Lebowitz, and Kalos [14] observed a linear force regime for weak forces and a Pincus-scaling [16] regime for large forces. The crossover region between both scaling regimes was found to be very narrow in contrast to first-order renormalization-group calculations given by Oono, Ohta, and Freed [15]. In a previous work [17] we studied both regimes and the crossover. We also found a rather narrow crossover regime, but this is in agreement with scaling functions obtained from more recent renormalization-group studies.

The inclusion of nonbonded intramolecular forces, usually assumed to be of van der Waals type, leads to a collapse transition when the temperature is lowered. At high temperatures or good solvent conditions the repulsive parts of the interaction (excluded volume) dominate, resulting in a swelling of the chain relative to a random coil. At low temperatures or poor solvent conditions on the other hand, monomer-monomer contacts become favorable and the chain tends to collapse into a compact dense globule. At an intermediate temperature, the Θ temperature T_Θ, the repulsive and attractive parts of the interaction cancel each other [18,19].

Regarding the deformation below the Θ temperature only a few works exist. These works indicate a deformation behavior completely different from that above T_Θ. Considering only surface energy terms, Halperin and Zhulina [20,21] proposed a linear force response for weak deformations and a constant force regime for intermediate stretching. The constant force regime involves a coexistence of a weakly deformed globular coil and a highly stretched strand. A more general description of the deformation behavior of a coil-strand system is the coil-strand-transition model [22,23], which was successfully used to describe crazes [23] and fibrils during the deformation of hard elastic polymers [24,25]. This model proposed a constant force regime too. With energy minimization techniques we studied in a previous paper [26] the deformation at zero temperature. These simulations showed clearly a coil-strand transition during stretching and a constant retractive force in this regime. Energy minimizations were also used to study the energy distribution in an extended chain under stress [27] and strain-induced conformational transitions [28]. Most recently Cifra and Bleha [29] discussed a bimodal shape of the end-to-end vector distribution function of stretched

chains below the Θ temperature. This bimodal shape indicates a coexistence of molecules in globular and extended coil formation. However, a complete investigation of the changes in deformation behavior changing the temperature from above to below T_Θ is outstanding.

A coil-strand formation is not quite unknown in the wide field of polymer physics. In extensional flows in dilute solutions there exists a transition to a stretched coil (cf. Frenkel [30]; a coil-stretch transition, cf. de Gennes [31]; and a "yo-yo" model, cf. Ryskin [32,33]), which also has been studied by computer simulations [34,35]. However, in these models the reason for the transition is the balance of the nonlinear stretching force due to the high gradients in the flow with the entropic retractive force, whereas in the present work nonbonded interactions lead to the coil-strand system. The possibility of forming coil-strand systems due to nonbonded forces can be seen in the work of Kavassalis and Sundararajan [36], who found such a behavior during a molecular-dynamics study of polyethylene crystallization. Similarities to a coil-strand formation can also be found when a polymer chain is pulled through a network with a certain velocity: the chain can be described by plume and sticklike regions [37].

On related topics computer simulations have shown their great possibilities to investigate elastic properties of polymers. Weiner and co-workers studied conformational transitions in an idealized polymer melt [38] and the behavior of tie molecules [39]. Termonia *et al.* developed a kinetic model for tensile deformation [40–42]. The mechanical properties of networks were studied extensively under various viewpoints (see Weiner and Stevens [43], Gao and Weiner [44–50], and Termonia [51–53]). Brown and co-workers performed a molecular-dynamics simulation of the deformation of polymer fiber microstructures [54] and of glasses [55,56] on short time scales. With energy minimization techniques the mechanical properties of certain polymers were computed by various authors (Suter and co-workers [57–62], Boyd and Pant [63,64], and Fan *et al.* [65,66]). Cook [67,68] investigated cold drawing at zero temperature. Dickman and Hong [69] computed the force between grafted polymeric brushes and Haliloglu, Behar, and Erman [70,71] studied oriental and conformational correlations in deformed chains.

The intention of this paper is to close the large gap between our previous works performed in the athermal limit of infinite temperature [17] and at zero temperature [26]. In the next section the simulation method will be described. The presentation of the results and a discussion will follow.

II. SIMULATION METHOD

Since we are not interested in chemical details of a certain polymer, we took advantage of the efficiency of a coarse-grained lattice model. The bond fluctuation model developed by Carmesin and Kremer [72] in three dimensions was taken. On a simple cubic lattice the monomers are represented by cubes of eight positions. The monomers are connected by a set of possible bond vectors (108 in three dimensions). The diffusion dynamic in the free draining limit is simulated by randomly chosen jumps of monomers in spatial directions. For more details on the bond fluctuation model we refer to the original papers [72–76].

In addition to the purely excluded-volume interaction, incorporated in the bond-fluctuation algorithm, we took into account a truncated Lennard-Jones potential $V(r)$ with a range of three grid units between all points of the monomers (r is the distance between the monomers) and a bond-length potential $V'(l)$ describing the increasing backbone stiffness with decreasing temperature:

$$V(r)=\frac{\epsilon}{2}\left\{\left[\frac{r}{r_0}\right]^{-12}-2\left[\frac{r}{r_0}\right]^{-6}\right\}, \tag{1}$$

$$V'(l)=\frac{\epsilon}{2}\left\{c_0+c_1\frac{l}{a}+c_2\left[\frac{l}{a}\right]^2+c_3\left[\frac{l}{a}\right]^3\right\}, \tag{2}$$

where ϵ is the unit of energy, $r_0=1.1a$, l is the bond length, and a is the lattice spacing. The parameters $c_0=-207.12$, $c_1=342.88$, $c_2=-163.52$, and $c_3=24.32$ were estimated from a static energy-minimization simulation, including ten unified polyethylene (PE) monomers interacting by bond-stretching, torsional, and van der Waals forces. The identification of a bond with a Kuhnian segment [2] of ten PE segments is somewhat arbitrary, but is in agreement with values used in the literature [77,78]. With this choice of parameters the chains are flexible in contrast to stiff chains; see Ref. [79]. At low temperatures long bonds are more likely leading to a higher acceptance rate within our model. Simulations of dense systems with the same parameters show that they can produce glassy samples [80]. The exact form of $V'(l)$ and the exact values of the constants have no influence on the qualitative results. Using the Metropolis criterion [81], the energies due to these potentials determined whether the jumps of monomers in our model were accepted.

There are two principal possibilities to perform a deformation experiment. One is to impose the force and measure the end-to-end distance in the force direction (stress ensemble) and the other is to increase the end-to-end distance in a certain direction and measure the retractive force in this direction (strain ensemble). We chose the second possibility since it is rather hard to study a constant force regime if one would impose the force. Weiner and Perchak [6] showed that there are differences between these two ensembles, but the differences vanish for chain lengths $N>6$. Within our model we changed the end-to-end distance R_f in the z direction and measured the retractive force fk_BT (k_B denotes Boltzmann's constant and T the temperature) by counting the tried jumps n_+ with $R_f\rightarrow R_f+a$ and n_- with $R_f\rightarrow R_f-a$. a is the lattice spacing. Then the force f, normalized by the temperature, was computed by

$$f=\frac{1}{a}\ln\frac{n_-}{n_+}. \tag{3}$$

We tested this method at temperatures above T_Θ by com-

paring the data with those obtained by imposing the force and found excellent agreement.

We studied single chains of $(N+1)=20$, 60, and 100 monomers on lattices with periodic boundary conditions. The lattice extensions were $20\times20\times50$ up to $56\times56\times176$. The dimensions of the lattices were large enough that interactions of the chain with itself over periodic boundary conditions can be neglected. To obtain proper statistics we performed 100–140 independent simulations.

A single simulation was done in the following manner: After creating the chains they were relaxed at least for 1000000 Monte Carlo steps (MCS). One MCS is one attempted jump per monomer. After this equilibration a continuous cooling process was started with the cooling rate $\Gamma_Q=4\times10^{-7}$ (MCS)$^{-1}$. Γ_Q denotes the reciprocal temperature step per time unit of the Monte Carlo simulation. The inverse temperature $\beta=1/k_BT$ at time t follows from $\beta\epsilon=\Gamma_Q t$. During cooling, configurations were extracted in intervals of $\Delta\beta\epsilon=0.05$ and afterward subjected to isothermal relaxation for a duration of 1 000 000 MCS. Then the measurements of the undeformed state were performed in intervals of 500 MCS for a total amount of 1 000 000 MCS. After that the deformation was started. First $R_f=0$ was imposed by applying a force at the chain until $R_f=0$ was reached. This configurations were equilibrated for 1 000 000 MCS. The distance R_f was then increased stepwise by an amount of $2a$. After each step a equilibration run was carried out for at least 150 000 MCS. Then the measurements were performed in intervals of 500 MCS for a total amount of 150 000 MCS. The data were averaged over the time and the independent simulations. We tested longer equilibration runs than 150 000 MCS after each strain step and found only slight differences. Thus 150 000 MCS is a sufficiently long time for the main part of the relaxation process after a strain step.

III. RESULTS AND DISCUSSION

A. Collapse transition

In order to characterize the undeformed state we give here a brief overview of the collapse transition. A detailed analysis of the collapse transition can be found in another paper [82].

In Fig. 1 we plotted the normalized mean square radius of gyration $\langle S_N^2\rangle/N$ versus the chain length n. The points represent the simulated data and the solid lines represent the limiting scaling laws $\sim N^{0.176}$ and $\sim N^{-1/3}$. In the infinite temperature limit (athermal limit $\beta\epsilon=0$) the chains are swollen, in agreement with the theory [83]. They obey the scaling law $\langle S_N^2\rangle\sim N^{2\nu_0}$, with $\nu_0=0.588\pm0.001$ [84].

With increasing β the curves become flatter, indicating the approach to the Θ point. At lower temperatures, higher β, than $\beta\epsilon=0.20$, $\langle S_N^2\rangle/N$ is no longer a linear function of N in the log-log-plot. This is due to the fact that the longest chains are already significantly collapsed, in contrast to the short chains. With decreasing chain

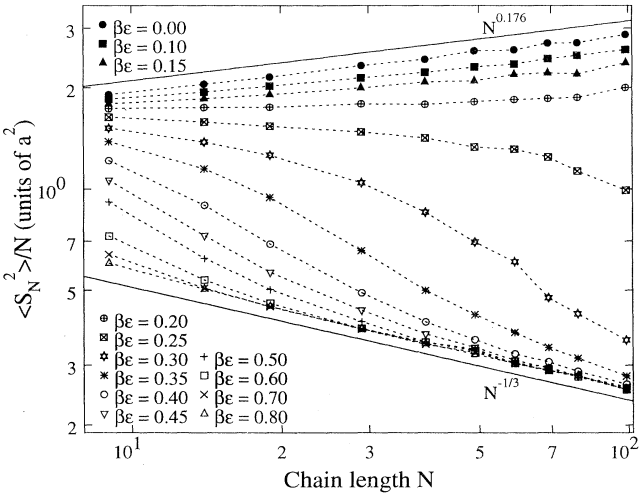

FIG. 1. log-log plot of $\langle S_N^2\rangle/N$ versus N for various temperatures. The points represent the simulated data and the dotted lines are guides to the eye. The solid lines represent $\sim N^{0.176}$ and $\sim N^{-1/3}$.

length N the temperature distance $T_\Theta-T$ from the Θ temperature must increase to obtain a significant collapse, i.e., $T_\Theta-T>T_\Theta/N^{1/2}$ [19,85]. The observed behavior is in accordance with other investigators; see, for example, the works by Kremer, Baumgärtner, and Binder [86] and Grassberger and Hegger [87].

At the lowest simulated temperatures ($\beta\epsilon>0.5$) also the short chains are fully collapsed and $\langle S_N^2\rangle$ scales according to the law $\langle S_N^2\rangle\sim N^{2\nu_c}$ with $\nu_c=\frac{1}{3}$ [19,83]. Thus the fully collapsed regime is reached and the chains are compact dense globules.

In order to determine the Θ temperature T_Θ we plotted in Fig. 2 $\langle S_N^2\rangle/N$ versus the inverse temperature $\beta\epsilon$. Since at the Θ temperature the chains behave as

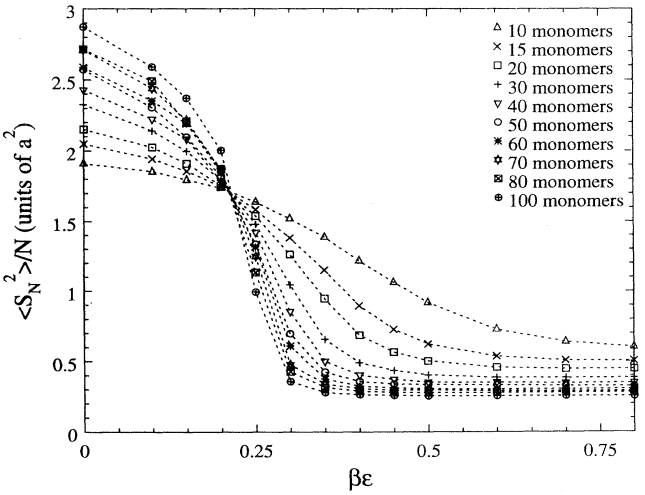

FIG. 2. Plot of $\langle S_N^2\rangle/N$ versus $\beta\epsilon$ for various chain lengths N. The points represent the simulated data and the dotted lines are guides to the eye.

$\langle S_N^2 \rangle \sim N$ (besides logarithmic corrections) [83] the curves for different N should intersect at β_Θ. The curves in Fig. 2 show a clear intersection point at $\beta_\Theta \epsilon = 1/(k_B T_\Theta) = 0.214 \pm 0.008$. This temperature is in good agreement with other methods to determine T_Θ as we pointed out in [82]. Moreover, it can be seen that the transition becomes sharper with increasing N, in agreement with other investigators [86–88].

B. Conformational changes

We now turn to the deformation behavior. To get a first impression of the conformational changes during deformation, Fig. 3 displays time shots of the shape of the deformed coil of a chain consisting of 100 monomers at $R_f/a = 0, 40, 80, 120, 160$. All conformations are plotted with the same scale. At $\beta\epsilon = 0$ [Fig. 3(a)] no prominent properties can be found, thus the deformation is homogeneous, as expected. At $\beta\epsilon = 0.3$ [Fig. 3(b)] the undeformed chain is collapsed since the temperature is below the Θ temperature. At $R_f = 40a$ a clear distinction between a stretched strand and a nearly unaltered residual coil can be seen. At higher strains the conformations are similar to those obtained above T_Θ. At $\beta\epsilon = 0.5$ the undeformed chain is fully collapsed, being a dense globule. The coil-strand coexistence can be observed for all R_f. The strand is in a more elongated conformation than at $\beta\epsilon = 0.3$. The deformation is obviously inhomogeneous. The coil-strand coexistence is in agreement with the ideas of Halperin and Zhulina [20,21] and the coil-strand-transition model [22,23]. To get a quantitative impression of the changes in the deformation behavior we analyze in the next subsection the dependence of the force on R_f.

C. Force dependence on the strain

Figures 4 and 5 display the achieved forces versus elongation of chains consisting of 20 and 100 monomers. The results for 60 monomers are in between.

At temperatures above the Θ temperature ($\beta_\Theta \epsilon = 0.214$) only slight differences to the infinite temperature limit $\beta\epsilon = 0$ (the athermal limit) occur. As we discussed in our previous paper [17], the behavior at $\beta\epsilon = 0$ can be described in the following way: for small strains ($R_f \ll \langle R_N^2 \rangle^{1/2}$) there is a linear response to the deformation, i.e., $\langle f \rangle = 3R_f/\langle R_N^2 \rangle$, where $\langle R_N^2 \rangle$ is the mean-square end-to-end distance of the undeformed chain. For intermediate strains the force scales with R_f as $\langle f \rangle \sim R_f^{3/2}$ [16,83]. Since the chain length is finite this scaling regime is only valid as long as $R_f \ll Nl$, where l is the length of a segment. Lowering the temperature to $\beta\epsilon = 0.2$ results in an increase of the linear force regime since at the Θ point the repulsive and attractive parts of the interaction cancel each other and the end-to-end distance distribution becomes very similar to a Gaussian distribution, as for random walks [82]. This is in agreement with the work of Webman, Lebowitz, and Kalos [14], who found that a chain at the Θ point obeys some ideal elastic properties. However, in this paper we concentrate on temperatures below T_Θ.

At temperatures below the Θ temperature the deformation behavior is completely different from that at $\beta\epsilon = 0$. At small strains the force rises nearly linearly to a high stress level. Then at larger R_f and $\beta\epsilon = 0.5$ a regime with constant force can be observed. This regime is characterized by the coil-strand coexistence, which can be seen in Fig. 3(c). The constancy of the force during the coil-strand coexistence is in agreement with the predic-

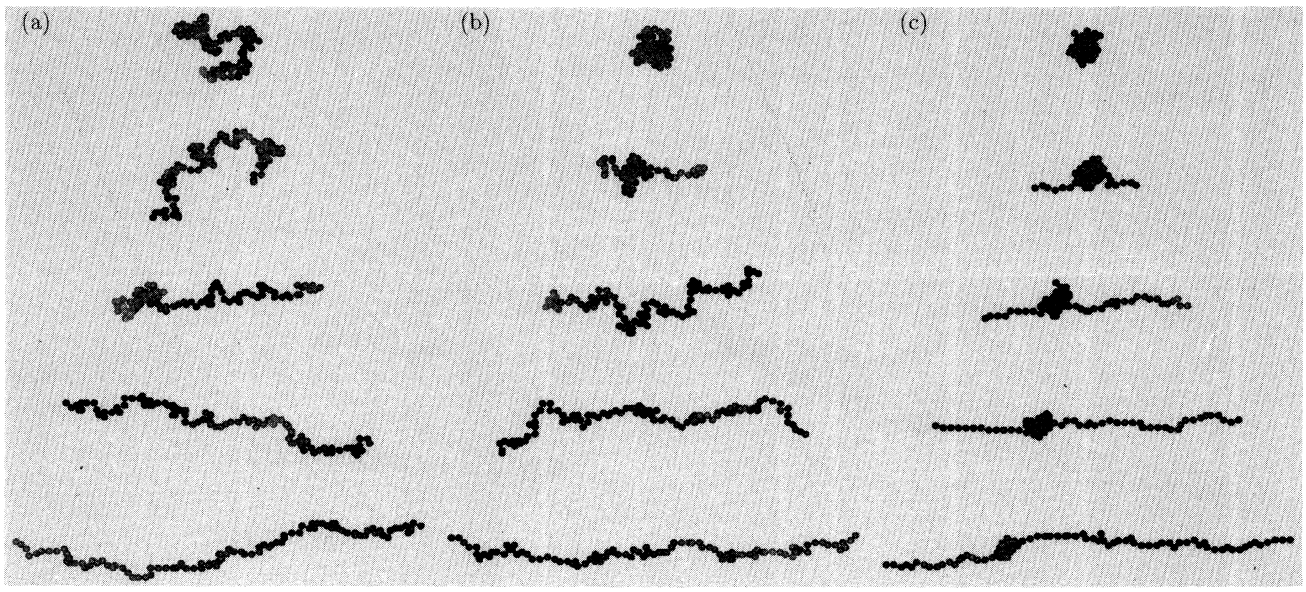

FIG. 3. Snapshots of the conformation of a coil consisting of 100 monomers for stretching steps $R_f/a = 0, 40, 80, 120, 160$: (a) $\beta\epsilon = 0$, (b) $\beta\epsilon = 0.3$, and (c) $\beta\epsilon = 0.5$. All conformations are plotted with the same scale.

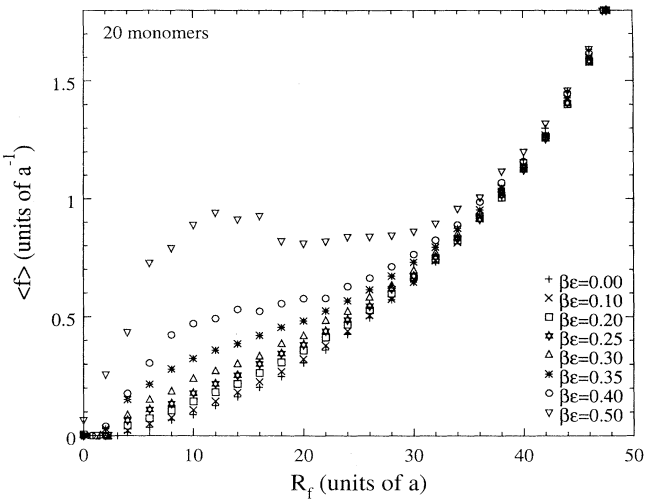

FIG. 4. Retractive force $\langle f \rangle$ versus end-to-end distance in force direction R_f for a chain consisting of 20 monomers at various temperatures.

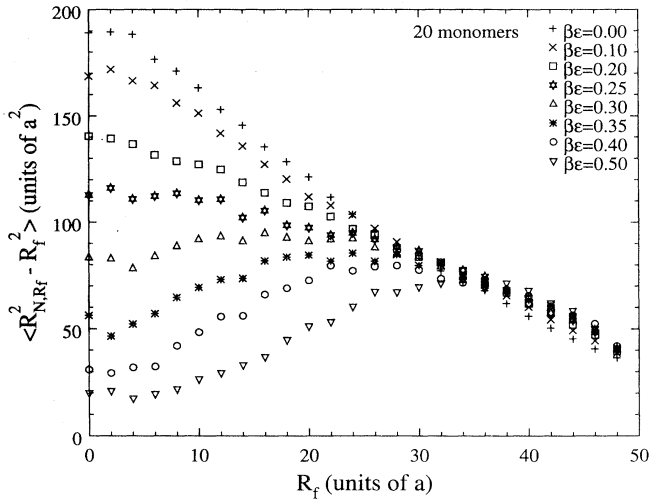

FIG. 6. Lateral spread $\langle R^2_{N,R_f} - R_f^2 \rangle$ versus end-to-end distance in force direction R_f for a chain consisting of 20 monomers at various temperatures.

tions of Halperin and Zhulina [20,21] and the coil-strand-transition model [22,23]. In the cases $\beta\epsilon = 0.25-0.4$ this regime is shorter or missing entirely. Because of the elongation the collapsed state is no longer stable at large R_f since the number of segments N_r in the residual coil decreases. The coil is only significantly collapsed as long as $T_\Theta - T > T_\Theta / N_r^{1/2}$ [19,85]. This can be already seen in Fig. 1, where for a given temperature only long enough chains reach the fully collapsed state with $\langle S_N^2 \rangle / N \sim N^{-1/3}$. Hence, at a certain R_f the coil-strand system becomes unstable and the deformation behavior approaches the behavior above T_Θ. Clearly, the elongation R_f where this happens decreases with decreasing chain length N and increasing temperature. This is in agreement with Halperin and Zhulina [20,21], who proposed that the end of the coexistence region should vary as $N(T_\Theta - T)/T_\Theta$. During the approach to the behavior above T_Θ the force even decreases with increasing R_f, as can be seen most pronounced in Fig. 5 at $\beta\epsilon = 0.35$. The change of an inhomogeneous deformed coil-strand system to a homogeneous deformed chain is displayed in Fig. 3(b). At $R_f = 40a$ a coil-strand system exists, which vanishes for larger R_f. On the other hand, the coil-strand coexistence is present over the whole deformation regime at $\beta\epsilon = 0.5$ [Fig. 3(c)].

D. Lateral spread

The change in the deformation behavior can be found in the variation of the mean-square end-to-end distance

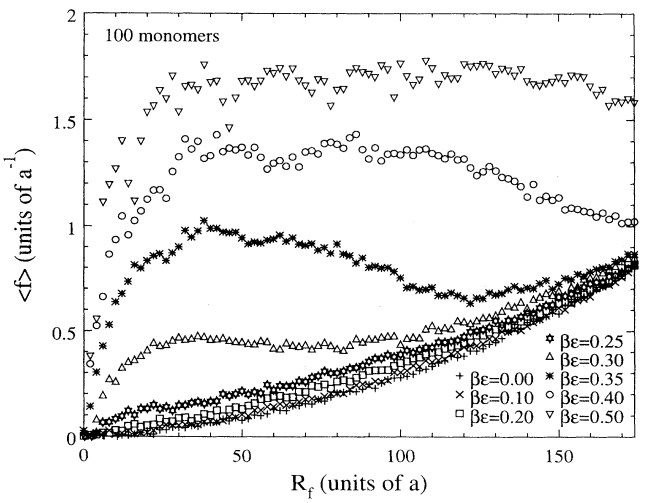

FIG. 5. Retractive force $\langle f \rangle$ versus end-to-end distance in force direction R_f for a chain consisting of 100 monomers at various temperatures.

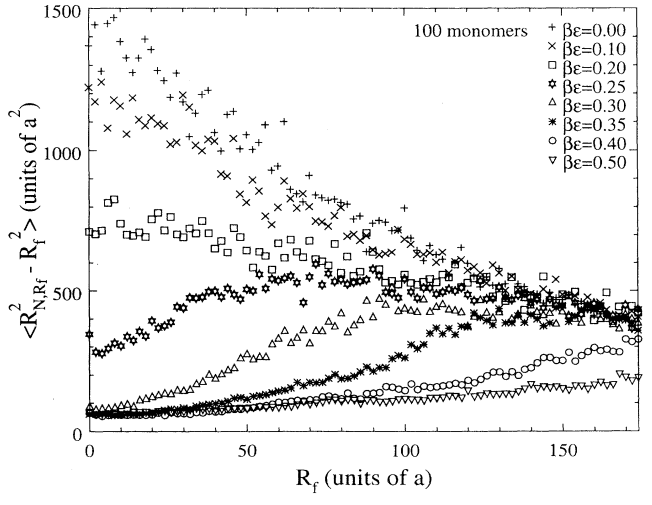

FIG. 7. Lateral spread $\langle R^2_{N,R_f} - R_f^2 \rangle$ versus end-to-end distance in force direction R_f for a chain consisting of 100 monomers at various temperatures.

$\langle R^2_{N,R_f} - R_f^2 \rangle$ perpendicular to the draw direction too. R_{N,R_f} is the total end-to-end distance of the chain, elongated to R_f. In Figs. 6 and 7 we plotted $\langle R^2_{N,R_f} - R_f^2 \rangle$ versus R_f for chains consisting of 20 and 100 monomers. Above the Θ temperature the lateral spread decreases with increasing strain for all R_f. This behavior change drastically when the temperature is lowered below T_Θ. The lateral spread $\langle R^2_{N,R_f} - R_f^2 \rangle$ increases with R_f up to the point where the curves of the chains at $T > T_\Theta$ are reached. Then $\langle R^2_{N,R_f} - R_f^2 \rangle$ exhibits the same behavior as above T_Θ, i.e., $\langle R^2_{N,R_f} - R_f^2 \rangle$ decreases with increasing R_f. In accordance with the discussion in Sec. III C, the value of R_f, where the curves coincide, decreases with decreasing β and N.

E. Variance of internal distances

In order to get a quantitative description of the conformational changes during deformation we calculated the variance of the internal distances: $\mathrm{Var}(R_n) = \langle R^2_{n,R_f} \rangle - \langle R_{n,R_f} \rangle^2$, where $R_{n,R_f} = |\vec{r}_i - \vec{r}_{i+n}|$ and $\vec{r}_i$ is the position of monomer i of the chain ($i = 0, 1, \ldots, N$). Besides the averaging over time and the independent simulations an averaging over i was performed. Figure 8 shows at three-dimensional plot of the variance of internal distances $\mathrm{Var}(R_n)$ as a function of the subchain length n and R_f for a chain consisting of 60 monomers: (a) $\beta\epsilon = 0$, (b) $\beta\epsilon = 0.2$, (c) $\beta\epsilon = 0.3$, (d) $\beta\epsilon = 0.35$, (e) $\beta\epsilon = 0.4$, and (f) $\beta\epsilon = 0.5$.

Above the Θ temperature [Figs. 8(a) and 8(b)] the vari-

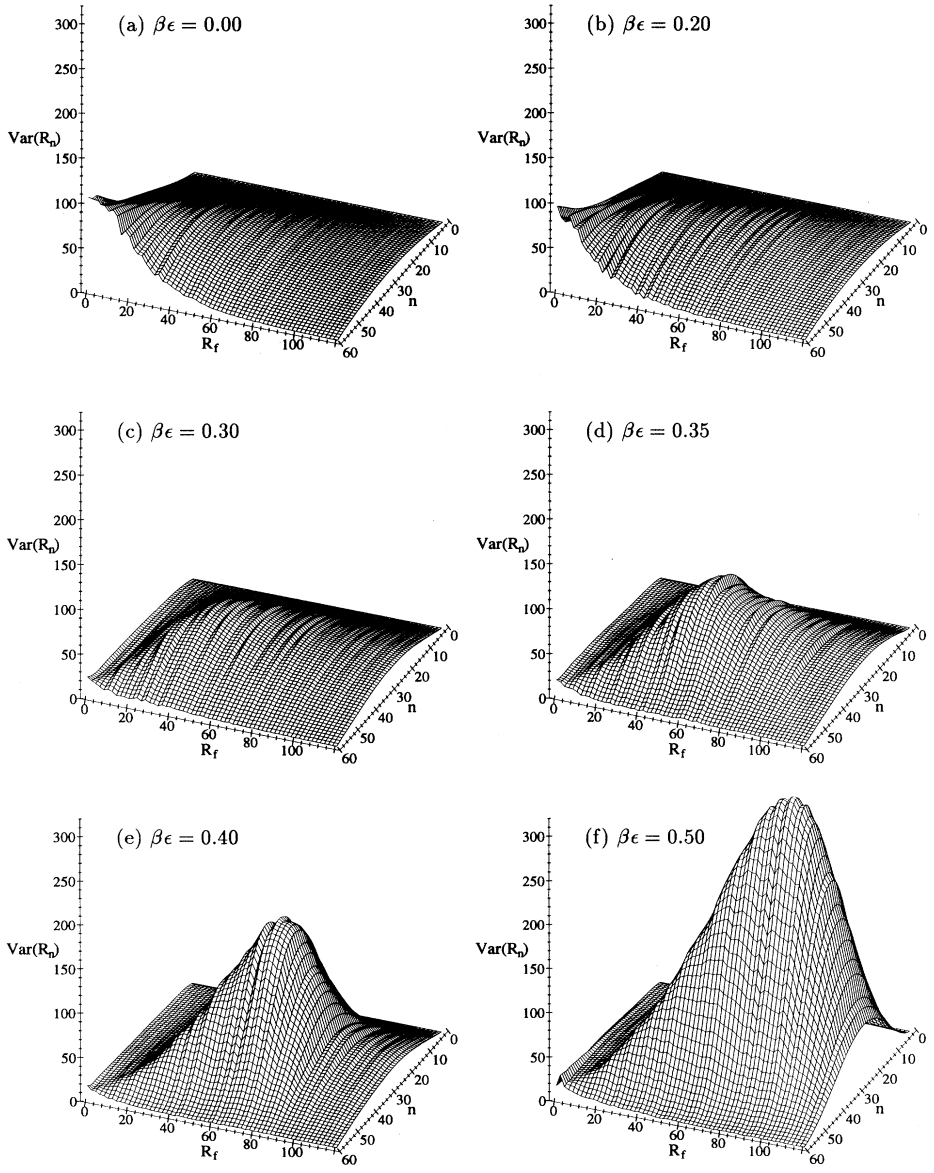

FIG. 8. Three-dimensional plot of the variance of internal distances, $\mathrm{Var}(R_n)$, as a function of the subchain length n and R_f for a chain consisting of 60 monomers: (a) $\beta\epsilon = 0$, (b) $\beta\epsilon = 0.2$, (c) $\beta\epsilon = 0.3$, (d) $\beta\epsilon = 0.35$, (e) $\beta\epsilon = 0.4$, and (f) $\beta\epsilon = 0.5$.

ance is maximal in the undeformed state ($R_f=0$) and for $n=N$ since there are fewer accessible distances for short subchains and $R_f=0$ does not restrict the accessible distances for R_{N,R_f} too much. With increasing R_f the variance for long subchains decreases since R_{N,R_f} gets locked at values close to R_f. Hence, for large R_f the variance becomes maximal for $n \approx N/2$.

Below the Θ temperature [Figs. 8(c)–8(f)] the chains are globules. Thus at $R_f=0$ the variance of all subchains is smaller than above T_Θ, particularly for long subchains. As above T_Θ, the variance for long subchains decreases with increasing R_f. However, at intermediate R_f a maximum around $n=N/2$ occurs, which becomes more prominent with decreasing temperature. This is a clear sign for the coil-strand coexistence. Some of the subchains are in the nearly unaltered residual coil having a smaller R_{n,R_f} than subchains in the strand. With decreasing temperature the residual globular coil becomes more compact and the strand more stretched (see also Fig. 3). Thus the difference between subchains in the coil and the strand increases leading to higher values of $\mathrm{Var}(R_n)$. For larger values of R_f the pronounced maximum disappears and the behavior of the variance becomes similar to that above T_Θ, indicating the disintegration of the coil-strand system. This changes take place at values of R_f in agreement with those where the force and the lateral spread are turning to the behavior above T_Θ, as discussed in the previous sections.

IV. SUMMARY AND CONCLUSION

Using the bond-fluctuation model we investigated the deformation behavior of a single polymer chain above and below the Θ temperature in three dimensions. Studying the conformational changes during the deformation, we found that above the Θ temperature no prominent properties can be seen, thus the deformation is homogeneous. In contrast to that below the Θ temperature, a clear distinction between a stretched strand and a nearly unaltered residual coil was observed, i.e., the deformation is inhomogeneous. At low temperatures this coil-strand coexistence was observed during a large extension range whereas at higher temperatures, but still below T_Θ, the coil-strand system disappeared at large strains.

The force dependence on the strain R_f showed only slight differences to the athermal limit as long as the temperature was above T_Θ. Below T_Θ a constant force regime was observed in the coil-strand coexistence regime. This is in agreement with the predictions of Halperin and Zhulina [20,21] and the coil-strand-transition model [22,23]. The range and existence of this regime depends on the temperature distance to T_Θ and the chain length N. It is more pronounced for low temperatures and long chains. This was interpreted in terms of an unstability of the coil-strand system caused by the elongation. Investigations of the lateral spreads and the variance of internal distances supported this viewpoint. In future work we plan to analyze the energetic and entropic parts during the creation and vanishing of the coil-strand system.

ACKNOWLEDGMENTS

Parts of the simulations were performed at the Leibniz Rechenzentrum der Bayerischen Akademie der Wissenschaften München, Höchstleistungsrechenzentrum für Wissenschaft und Forschung KFA Jülich, and on the facilities of the Rechenzentrum der Universität Regensburg. We are grateful for a generous grant of computing time. Moreover, M.W. would like to thank the Deutsche Forschungsgemeinschaft for financial support (Grant No. Go 287/18-1).

[1] W. Kuhn, Kolloid Z. **68**, 2 (1934).
[2] W. Kuhn and F. Grün, Kolloid Z. **101**, 248 (1942).
[3] P. J. Flory, *Statistical Mechanics of Chain Molecules* (Interscience, New York, 1969).
[4] J. H. Weiner and D. Perchak, Macromolecules **14**, 1590 (1981).
[5] J. H. Weiner, Macromolecules **15**, 542 (1982).
[6] D. Perchak and J. H. Weiner, Macromolecules **15**, 545 (1982).
[7] J. H. Weiner and D. H. Berman, J. Chem. Phys. **82**, 548 (1985).
[8] J. H. Weiner and D. H. Berman, J. Polym. Sci. Polym. Phys. **24**, 389 (1986).
[9] H. Davis, Macromolecules **28**, 1060 (1995).
[10] A. R. Altenberger, E. Rosa, and J. S. Dahler, J. Chem. Phys. **100**, 3233 (1994).
[11] G. Glatting, R. G. Winkler, and P. Reineker, Macromolecules **26**, 6085 (1993).
[12] G. Glatting, R. G. Winkler, and P. Reineker, Macromol. Theory Simul. **3**, 575 (1994).
[13] G. Glatting, R. G. Winkler, and P. Reineker, Colloid Polym. Sci. **273**, 32 (1995).
[14] I. Webman, J. L. Lebowitz, and M. H. Kalos, Phys. Rev. A **23**, 316 (1981).
[15] Y. Oono, T. Ohta, and K. F. Freed, Macromolecules **14**, 880 (1981).
[16] P. Pincus, Macromolecules **9**, 386 (1976).
[17] M. Wittkop, J.-U. Sommer, S. Kreitmeier, and D. Göritz, Phys. Rev. E **49**, 5472 (1994).
[18] P. J. Flory, *Principles of Polymer Chemistry* (Cornell University Press, Ithaca, 1967).
[19] C. Williams, F. Brochard, and H. L. Frisch, Annu. Rev. Phys. Chem. **32**, 433 (1981).
[20] A. Halperin and E. B. Zhulina, Europhys. Lett. **15**, 417 (1991).
[21] A. Halperin and E. B. Zhulina, Macromolecules **24**, 5393 (1991).
[22] D. Göritz, S. Kreitmeier, and M. Wittkop, J. Macromol. Sci. Phys. (to be published).
[23] S. Kreitmeier and D. Göritz, Makromol. Chem. Macromol. Symp. **41**, 253 (1991).
[24] M. Wittkop, S. Kreitmeier, and D. Göritz, Acta Polym. **46**, 319 (1995).
[25] S. Kreitmeier, M. Wittkop, T. Wagner, D. Göritz, and R.

Zietz, Colloid Polym. Sci. (to be published).
[26] S. Kreitmeier, M. Wittkop, and D. Göritz, J. Comput. Phys. **112**, 267 (1994).
[27] T. Bleha and J. Gajdos, Colloid Polym. Sci. **266**, 405 (1988).
[28] T. Bleha, J. Gajdos, and F. E. Karasz, Macromolecules **23**, 4076 (1990).
[29] P. Cifra and T. Bleha, Macromol. Theory Simul. **4**, 233 (1995).
[30] J. Frenkel, Acta Physicochim. USSR **19**, 51 (1944).
[31] P. G. de Gennes, J. Chem. Phys. **60**, 5030 (1974).
[32] G. Ryskin, J. Fluid. Mech. **178**, 423 (1987).
[33] G. Ryskin, Phys. Rev. Lett. **59**, 2059 (1987).
[34] R. G. Larson and J. J. Magda, Macromolecules **22**, 3004 (1989).
[35] R. G. Larson, Rheol. Acta **29**, 371 (1990).
[36] T. A. Kavassalis and P. R. Sundararajan, Macromolecules **26**, 4144 (1993).
[37] J. M. Deutsch and H. Yoon, J. Chem. Phys. **102**, 7251 (1995).
[38] J. H. Weiner and M. R. Pear, Macromolecules **20**, 317 (1977).
[39] J. H. Weiner and D. H. Berman, Macromolcules **17**, 2015 (1984).
[40] Y. Termonia and P. Smith, Macromolecules **20**, 835 (1987).
[41] Y. Termonia and P. Smith, Macromolecules **21**, 2184 (1988).
[42] Y.Termonia, S.R. Allen, and P. Smith, Macromolecules **21**, 2184 (1988).
[43] J. H. Weiner and T. W. Stevens, Macromolecules **16**, 672 (1983).
[44] J. Gao and J. H. Weiner, Macromolecules **20**, 2520 (1987).
[45] J. Gao and J. H. Weiner, Macromolcules **20**, 2625 (1987).
[46] J. Gao and J. H. Weiner, Macromolecules **21**, 773 (1988).
[47] J. Gao and J. H.Weiner, Macromolecules **22**, 979 (1989).
[48] J. Gao and J. H. Weiner, J. Chem. Phys. **90**, 6749 (1989).
[49] J. Gao and J. H. Weiner, Macromolecules **24**, 1519 (1991).
[50] J. Gao and J. H.Weiner, Macromolecules **24**, 5179 (1991).
[51] Y. Termonia, Macromolecules **22**, 3633 (1989).
[52] Y. Termonia, Macromolecules **23**, 1481 (1990).
[53] Y. Termonia, Macromolecules **23**, 1976 (1990).
[54] D. Brown and J. H. R. Clarke, J. Chem. Phys. **84**, 2858 (1986).
[55] D. Brown and J. H. R. Clarke, Macromolecules **24**, 2075 (1991).
[56] J. I. McKechnie, R. N. Haward, D. Brown, and J. H. R. Clarke, Macromolecules **26**, 198 (1993).
[57] D. N. Theodorou and U. W. Suter, Macromolecules **19**, 139 (1986).
[58] D. N. Theodorou and U. W. Suter, Macromolecules **19**, 379 (1986).
[59] A. S. Argon, P. H. Mott, and U. W. Suter, Phys. Status Solidi B **172**, 193 (1992).
[60] P. H. Mott, A. S. Argon, and U. W. Suter, Philos. Mag. A **67**, 931 (1993).
[61] P. H. Mott, A. S. Argon, and U. W. Suter, Philos. Mag. A **68**, 537 (1993).
[62] M. Hutnik, A. S. Argon, and U. W. Suter, Macromolecules **26**, 1097 (1993).
[63] R. H. Boyd and P. V. K. Pant, Macromolecules **24**, 4073 (1991).
[64] R. H. Boyd and P. V. K. Pant, Macromolecules **24**, 4078 (1991).
[65] C. F. Fan and S. L. Hsu, Macromolecules **25**, 266 (1992).
[66] C. F. Fan, T. Çağin, Z. M.Chen, and K. A. Smith, Macromolecules **27**, 2383 (1994).
[67] R. Cook, J. Polym. Sci. Polym. Phys. **26**, 1337 (1988).
[68] R. Cook, J. Polym. Sci. Polym. Phys. **26**, 1349 (1988).
[69] R. Dickman and D. C. Hong, J. Chem. Phys. **95**, 4650 (1991).
[70] T. Haliloglu, I. Behar, and B. Erman, J. Chem. Phys. **97**, 4428 (1992).
[71] T. Haliloglu, I. Behar, and B. Erman, J. Chem. Phys. **97**, 4438 (1992).
[72] I. Carmesin and K. Kremer, Macromolecules **21**, 2819 (1988).
[73] I. Carmesin and K. Kremer, J. Phys. (Paris) **51**, 915 (1990).
[74] A. L. Rodriguez, H.-P. Wittmann, and K. Binder, Macromolecules **23**, 4327 (1990).
[75] H.-P. Deutsch and K. Binder, J. Chem. Phys. **94**, 2294 (1991).
[76] H.-P. Wittmann, K. Kremer, and K. Binder, J. Chem. Phys. **96**, 6291 (1992).
[77] J. Baschnagel, K. Binder, W. Paul, M. Laso, U. W. Suter, I. Batoulis, W. Jilge, and T. Bürger, J. Chem. Phys. **95**, 6014 (1991).
[78] J. Baschnagel, K. Qin, W. Paul, and K. Binder, Macromolecules **25**, 3117 (1992).
[79] A. Kolinski, J. Skolnick, and R. Yaris, J. Chem. Phys. **85**, 3485 (1986).
[80] M. Wittkop, T. Hölzl, S. Kreitmeier, and D. Göritz (unpublished).
[81] N. Metropolis, A. W. Rosenbluth, M. N. Rosenbluth, A. H. Teller, and E. Teller, J. Chem. Phys. **21**, 1087 (1953).
[82] M. Wittkop, S. Kreitmeier, and D. Göritz, J. Chem. Phys. (to be published).
[83] P. G. de Gennes, *Scaling Concepts in Polymer Physics* (Cornell University Press, Ithaca, 1979).
[84] J. C. Le Guillou and J. Zimm-Justin, Phys. Rev. Lett. **38**, 95 (1977).
[85] P. G. de Gennes, J. Phys. (Paris) Lett. **46**, L639 (1985).
[86] K. Kremer, A. Baumgärtner, and K. Binder, J. Phys. A **15**, 2879 (1981).
[87] P. Grassberger and R. Hegger, J. Chem. Phys. **102**, 6881 (1995).
[88] I. Webman, J. L. Lebowitz, and M. H. Kalos, Macromolecules **14**, 1495 (1981).

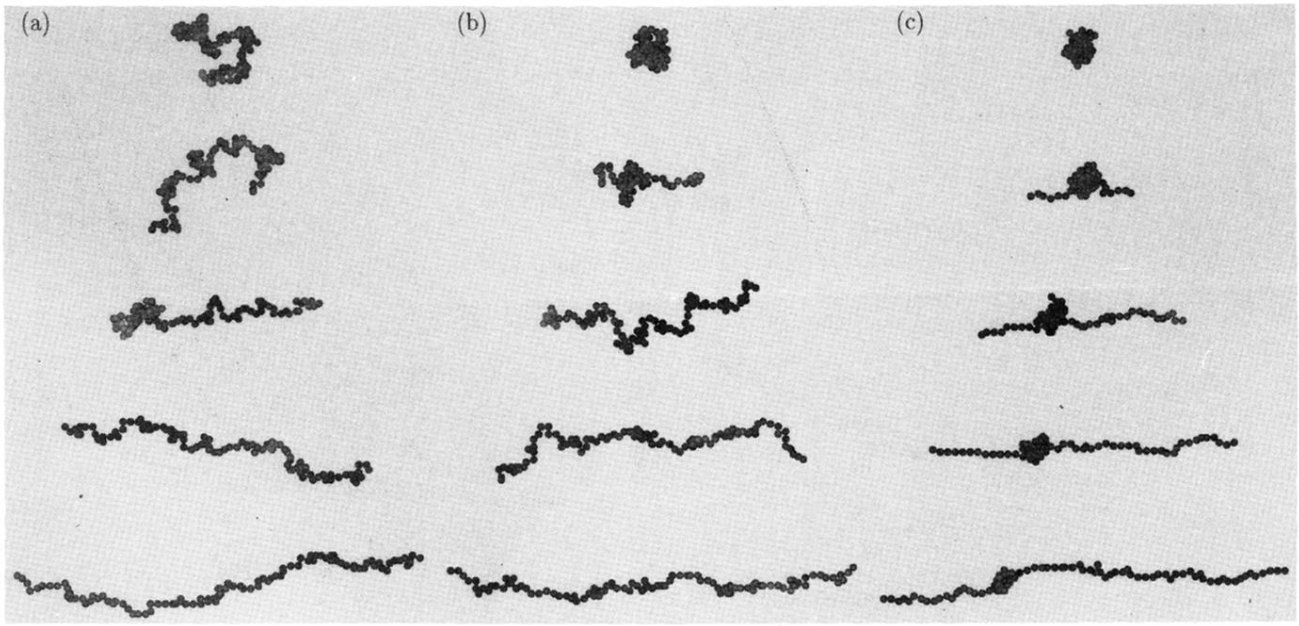

FIG. 3. Snapshots of the conformation of a coil consisting of 100 monomers for stretching steps $R_f/a = 0, 40, 80, 120, 160$: (a) $\beta\epsilon = 0$, (b) $\beta\epsilon = 0.3$, and (c) $\beta\epsilon = 0.5$. All conformations are plotted with the same scale.